HHS Public Access

Author manuscript

Circulation. Author manuscript; available in PMC 2020 September 10.

Published in final edited form as:

Circulation. 2019 September 10; 140(11): 921–936. doi:10.1161/CIRCULATIONAHA.118.034731.

Polycystin-1 assembles with Kv channels to govern cardiomyocyte repolarization and contractility

Francisco Altamirano, PhD[1], **Gabriele G. Schiattarella, MD, PhD**[1,5], **Kristin M. French, PhD**[1], **Soo Young Kim, MSc**[1], **Felipe Engelberger**[4], **Sergii Kyrychenko, PhD**[1], **Elisa Villalobos, PhD**[1], **Dan Tong, MD, PhD**[1], **Jay W. Schneider, MD, PhD**[1], **Cesar A. Ramirez-Sarmiento, PhD**[4], **Sergio Lavandero, PhD**[1,3], **Thomas G. Gillette, PhD**[1], **Joseph A. Hill, MD, PhD**[1,2,§]

[1]Department of Internal Medicine (Cardiology Division), University of Texas Southwestern Medical Center, Dallas, TX 75390-8573, USA

[2]Department of Molecular Biology, University of Texas Southwestern Medical Center, Dallas, TX 75390-8573, USA

[3]Advanced Center for Chronic Diseases (ACCDiS), Facultad de Ciencias Químicas y Farmacéuticas & Facultad de Medicina, Universidad de Chile, Santiago 8380492, Chile

[4]Institute for Biological and Medical Engineering, Schools of Engineering, Medicine and Biological Sciences, Pontificia Universidad Catolica de Chile, Santiago 7820436, Chile.

[5]Department of Advanced Biomedical Sciences, Federico II University, Naples 80131, Italy

Abstract

Background—Polycystin-1 (PC1) is a transmembrane protein originally identified in autosomal dominant polycystic kidney disease (ADPKD) where it regulates the calcium-permeant cation channel polycystin-2. ADPKD patients develop renal failure, hypertension, left ventricular hypertrophy, atrial fibrillation, among other cardiovascular disorders. These individuals harbor PC1 loss-of-function mutations in their cardiac myocytes, but the functional consequences are unknown. PC1 is ubiquitously expressed, and its experimental ablation in cardiomyocyte-specific knockout mice reduces contractile function. Here, we set out to determine the pathophysiological role of PC1 in cardiomyocytes.

Methods—WT and cardiomyocyte-specific PC1 KO mice were analyzed by echocardiography. Excitation-contraction coupling was assessed in isolated cardiomyocytes and hESC-derived cardiomyocytes, and functional consequences were explored in heterologous expression systems. Protein-protein interactions were analyzed biochemically and by means of *ab initio* calculations.

Results—PC1 ablation reduced action potential duration (APD) in cardiomyocytes, decreased Ca^{2+} transients, and myocyte contractility. PC1-deficient cardiomyocytes manifested a reduction in SR Ca^{2+} stores due to a reduced APD and SERCA activity. An increase in outward K^{+} currents decreased APD in cardiomyocytes lacking PC1. Over-expression of full-length PC1 in HEK293

[§]**Correspondence to:** Joseph A. Hill, MD, PhD, Department of Internal Medicine (Cardiology), University of Texas Southwestern Medical Center, 6000 Harry Hines Blvd, Dallas, TX 75390-8573, USA. joseph.hill@utsouthwestern.edu, Phone: 214-648-1400.

DISCLOSURES

None.

cells significantly reduced the current density of heterologously expressed Kv4.3, Kv1.5 and Kv2.1 channels. PC1 C-terminus inhibited Kv4.3 currents to the same degree as full-length PC1. Additionally, PC1 co-immunoprecipitated with Kv4.3, and a modeled PC1 C-terminal structure suggested the existence of two docking sites for PC1 within the N-terminus of Kv4.3, supporting a physical interaction. Finally, a naturally occurring human mutant $PC1^{R4228X}$ manifested no suppressive effects on Kv4.3 channel activity.

Conclusions—Our findings uncover a role for PC1 in regulating multiple Kv channels, governing membrane repolarization and alterations in SERCA that reduce cardiomyocyte contractility.

Keywords

Voltage-gated K^+ channels; contractility; calcium; action potential; Kv4.3; Kv1.5; Kv2.1; L-type calcium channels; ryanodine receptor

INTRODUCTION

Autosomal-dominant polycystic kidney disease (ADPKD), the most common form of polycystic kidney disease (PKD), is a progressive renal disorder with adult onset.[1] The disease occurs worldwide with an estimated prevalence of 1:400–1,000 and is characterized by progressive nephropathy that accounts for 4–10% of patients with end-stage renal disease.[2] Cardiovascular disorders are the major complication contributing to both morbidity and mortality in patients with PKD.

Mutations in the genes (*PKD1* and *PKD2*) encoding polycystin-1 (PC1) and −2 (PC2) underlie ADPKD. Impairment of either PC1- or PC2-dependent signaling leads to fluid-filled renal cysts, deteriorating kidney function, and ultimately, renal failure.[2] ADPKD patients present with multiple cardiovascular conditions, including susceptibility to atrial fibrillation, hypertension, left ventricular hypertrophy, diastolic dysfunction, cardiac valvular disease, aortic root dilatation, arterial aneurysms/dissections, and pericardial effusion.[3] The extent to which these abnormalities stem from the effects of comorbidities impinging on the heart versus cardiomyocyte-autonomous actions of mutant polycystin proteins is unknown.

Present thinking holds that cardiovascular dysfunction in ADPKD patients stems from chronic hypertension and progressive kidney dysfunction. Positive correlation between hypertension and cardiac hypertrophy suggests that dysfunction arises mainly from hypertensive complications.[4] However, left ventricular hypertrophy and diastolic dysfunction can manifest during childhood or in young adults prior to a formal diagnosis of hypertension, suggesting that other events contribute[5–7]. Interestingly, the coexistence of ADPKD and cardiomyopathy appears to be higher than expected by chance[3], and evidence suggests that left ventricular contractile function is impaired in ADPKD patients with normal or moderately reduced kidney function.[8] Given this, it is imperative to parse the roles of cues emanating from outside the heart and those occurring from within the cardiomyocyte itself.

Results from our group show that *Pkd2* deletion, exclusively in cardiomyocytes, does not affect systolic nor diastolic function.[9] This evidence suggests that *Pkd2* deletion in cardiomyocytes is not enough to produce cardiac dysfunction, and alterations observed with organism-wide *Pkd2* haploinsufficiency may be triggered by other mechanisms.[10, 11] Some evidence suggests that mechanical stress triggers PC1-dependent activation of polycystin-2 (PC2), as seen in primary cilia in renal epithelial cells. This allows the primary cilia to act as a flow sensor by eliciting Ca^{2+} influx via PC2.[12] Co-assembly of both proteins generates cation-permeable currents that elicit increases in intracellular Ca^{2+}.[13] That said, it is debated whether this Ca^{2+} influx is responsible for mechanosensation in primary cilia.[14] In other cell types, PC1 participates in a variety of signaling pathways involved in cell proliferation, tubulogenesis, flow sensing, metabolism, cell death, and autophagy.[15]

Despite a large literature describing PC1 functions, little is known about molecular mechanisms governing its actions. We recently showed that *Pkd1* silencing in cardiomyocytes blunted hypertrophic growth triggered by pressure overload stress, providing evidence for a role for PC1 in stabilizing L-type Ca^{2+} channel (LTCC) protein.[16] In addition, we observed mild systolic dysfunction after *Pkd1* silencing. Here, we performed detailed characterization of cardiac contractile function and electrophysiological events in cardiomyocyte-specific PC1 KO mice with a goal of defining molecular mechanisms of PC1 action.

METHODS

All data, analytic methods, and study materials will be made available to other researchers on reasonable request for purposes of reproducing our results or replicating the procedures. Detailed materials and methods are in the online-only Data Supplement.

Animals

All procedures were approved by the Institutional Animal Care and Use Committee at the University of Texas Southwestern Medical Center.

Quantification and statistical analysis

Data are presented as mean ± SEM. Detailed information regarding sample sizes and data collection are indicated in each figure and figure legend. Data were analyzed either by the unpaired *t*-test to compare means when there were two experimental groups or by one-way ANOVA followed by Dunnette's post-test to compare means among ≥3 groups. A paired *t*-test was used for AP-clamp experiments in adult/hESC-derived cardiomyocytes, because they were applied on the same cell. Data were analyzed statistically with GraphPad Prism 7.03 (GraphPad Software, Inc.) and OriginPro 2017 (64-bit) SR2 (OriginLab Corporation). Differences were considered significant at $P<0.05$. Detailed information, including blinded experiments, are in the online-only Data Supplement.

RESULTS

Cardiomyocyte-specific *Pkd1* deletion diminishes myocardial contractile function

Given our prior findings of PC1-dependent stabilization of LTCC protein[16], we set out to define mechanisms of PC1 control of cardiomyocyte transmembrane ion channels. First, we studied mice conditionally silenced for PC1 selectively in cardiomyocytes. By crossing mice harboring floxed *Pkd1* alleles (*Pkd1*$^{f/f}$) in the presence or absence of a Cre transgene expressed under the control of the cardiomyocyte-specific promoter αMHC (*αMHC-Cre*), we engineered a cardiomyocyte-specific PC1 KO mouse (*αMHC-Cre*;*Pkd1*$^{f/f}$) (Supplemental Figure 1A–B). The resulting *Pkd1*$^{f/f}$ and *αMHC-Cre*;*Pkd1*$^{f/f}$ animals are referred to herein as F/F and PC1 cKO mice, respectively.

Adult cardiomyocytes isolated from PC1 cKO mice manifested nearly 100% recombination between flox sites, as well as reduced *Pkd1* mRNA and protein levels (Supplemental Figure 1C–E). In line with our previous results[16], PC1 cKO mice manifested reduced ventricular systolic function without sign of basal hypertrophy, compared with F/F mice, as assessed by echocardiography (Figure 1A–E and Supplemental Table 1). In addition, we detected profound diastolic dysfunction in PC1 cKO mice compared to control mice, measured as E/A (pulse wave Doppler) and E/e' (tissue Doppler) ratios (Figure 1F–H and Supplemental Table 2). To determine whether the contractile dysfunction was specific to PC1 ablation, we studied WT mice (C57BL/6) expressing Cre (*αMHC-Cre*). We did not observe differences in contractile function between WT and WT *αMHC-Cre* animals (Supplemental Figure 2).

To dissect mechanisms underlying contractile dysfunction in PC1-deficient hearts, we first measured changes in sarcomere length elicited by field electrical stimulation in isolated cardiomyocytes. Isolated adult mouse ventricular myocytes were paced with field electrical stimulation, and changes in sarcomere length were measured using an IonOptix imaging system. PC1 cKO cardiomyocytes manifested a decreased peak of contraction with slower kinetics of both contraction and relaxation compared with F/F cardiomyocytes (Figure 1I–N). We did not observe contractility changes elicited by the αMHC-Cre transgene in the WT background (Supplemental Figure 3). Together, these data highlight the importance of PC1 to maintain myocardial contractile performance, both in systole and in diastole, under resting conditions.

Cardiomyocyte action potential is altered by PC1 ablation

Cardiomyocyte contractions are triggered by an action potential (AP) that propagates into invaginations of the plasmalemma called T-tubules. Membrane depolarization promotes Ca^{2+} entry through LTCC and the subsequent Ca^{2+}-induced Ca^{2+} release by type 2 ryanodine receptors (RyR2) in a process known as excitation-contraction coupling (ECC) (Figure 2A). To unveil molecular mechanisms responsible for contractility alterations in PC1 cKO cardiomyocytes, we measured key components of the ECC process.

We measured APs by whole-cell current clamp. PC1 cKO cardiomyocytes exhibited substantially shorter APs compared to control cardiomyocytes (Figure 2B–D). No differences were observed in AP peak amplitude, maximum upstroke slope or resting membrane potential across the genotypes, pointing to a likely repolarization defect (Figure

2E–G). Consistent with the shortened AP duration, we observed significant shortening of QT intervals in PC1 cKO mice in surface electrocardiogram recordings (Figure 2H–I). No changes in heart rate were observed across the genotypes. In aggregate, these data point to a model in which PC1 plays a critical role in AP duration under normal physiologic conditions likely at the level of AP repolarization.

To evaluate cellular structure, we used confocal microscopy and the potentiometric dye Fluovolt™ to collect fluorescence images from adult cardiomyocytes isolated from F/F and PC1 cKO mice. The T-tubule network was assessed using Auto-TT Software.[17] No differences were observed across the genotypes, suggesting normal T-tubule architecture in PC1-deficient cardiomyocytes (Figure 2J–K).

Ca^{2+} cycling is impaired in cardiomyocytes lacking PC1

Next, we evaluated Ca^{2+} transients during pacing using Fura-2AM and an IonOptix fluorescence detection system. Cells were paced with 25–30 pulses at a frequency of 1 Hz and then, quickly stimulated with caffeine to quantify SR Ca^{2+} stores (Figure 3A). Quantification was performed during steady state using the average of the last 10 Ca^{2+} transients. Smaller and slower Ca^{2+} transients were observed in PC1 cKO cardiomyocytes compared to F/F counterparts (Figure 3B–G). No changes in time to peak or diastolic calcium were observed. We confirmed these findings in neonatal rat ventricular myocytes (NRVM) pre-treated with siRNA targeting *Pkd1* mRNA (Supplemental Figure 4). *Pkd1* mRNA decreased by 90% after 72 h of PC1 siRNA transfection compared to control siRNA (Supplemental Figure 4A). Ca^{2+} transient amplitude was significantly reduced in cardiomyocytes transfected with PC1 siRNA compared to control siRNA (Supplemental Figure 4B–D), confirming that PC1 ablation is directly responsible for these alterations rather than their arising as a secondary response in PC1 cKO cardiomyocytes.

We studied the response to frequency stimulation in PC1 cKO cardiomyocytes. We measured both contractility and Ca^{2+} transients in adult mouse cardiomyocytes electrically stimulated at 0.5, 1, 2, and 4 Hz (Supplemental Figure 5A–B). Consistent with our observations in cardiomyocytes paced at 1 Hz, PC1-deficient cardiomyocytes manifested both reduced Ca^{2+} transients and suppressed contractility compared to F/F controls at all frequencies studied (Supplemental Figure 5C–D). Together, these results suggest that cardiac dysfunction observed in PC1 cKO is caused by alterations in Ca^{2+}-cycling.

Caffeine-induced Ca^{2+} transients revealed a reduction in SR Ca^{2+} stores in PC1 cKO cardiomyocytes after steady-state pacing (Figure 3H). Using the decay constants from the Ca^{2+} transients (1 Hz and caffeine), we estimated NCX extrusion and SERCA uptake rates. A significant reduction in SERCA activity (17%) with no changes in NCX extrusion rates was observed in PC1 cKO cardiomyocytes (Figure 3I–J). These results suggest that slower Ca^{2+} transient decay is caused by reduced SERCA activity in PC1-deficient cardiomyocytes. Then, we measured SR Ca^{2+} stores under resting conditions for both F/F and PC1 cKO cardiomyocytes. No differences in SR Ca^{2+} stores were observed among genotypes (Supplemental Figure 6A–B). These data suggest that no alterations in RyR activation exist and that SR Ca^{2+} stores can potentially load to the similar extent in PC1 cKO cardiomyocytes; during pacing, however, SR Ca^{2+} content does not reach normal levels.

Then, we studied whether LTCC currents ($I_{Ca,L}$) are impaired in PC1-deficient cardiomyocytes. No differences were found in $I_{Ca,L}$ across the examined genotypes (Figure 3K and Supplemental Figure 6C–G), suggesting normal activation of these channels in PC1 cKO cardiomyocytes.

AP duration can determine the time course of $I_{Ca,L}$, resulting in changes in SR Ca^{2+} loading, SR Ca^{2+} release and contractility.[18] We therefore hypothesized that the Ca^{2+} alterations observed in PC1 cKO cardiomyocytes stem from changes in AP duration. To test this, we used the representative AP recordings obtained from F/F and PC1 cKO mice (Figure 2B) to perform AP-clamps in WT (F/F) adult cardiomyocytes. Using whole-cell voltage clamp, we imposed F/F or PC1 cKO AP waveforms (20 AP at 1 Hz) and measured the resulting Ca^{2+} transient in the same cardiomyocyte. The PC1 cKO AP waveform generated smaller Ca^{2+} transients compared to a F/F AP waveform (Figure 3L–N).

To parse the contributions of alteration in AP duration and SERCA activity, we used a depolarizing pulse at +10 mV and evaluated the Ca^{2+} response at a fixed stimulation time and potential. Interestingly, square pulse stimulation (20 pulses at 1 Hz) elicited similar responses in both F/F and PC1 cKO cardiomyocytes in terms of Ca^{2+} transient amplitude (Figure 3O–P). However, transient decay was still slower in PC1 cKO cardiomyocytes (Figure 3Q). We corroborated these data by raising extracellular K^+ to change the equilibrium potential for K^+ and trigger cardiomyocyte depolarization, evoking intracellular Ca^{2+} transients. Chemical depolarization triggered Ca^{2+} transients in PC1 cKO cardiomyocytes indistinguishable from WT cells, consistent with our hypothesis (Supplemental Figure 6H–I). In addition, contractility (sarcomere length) and Ca^{2+} dynamics (Fura-2AM) were assessed simultaneously using IonOptix technology. As expected, both cardiomyocyte contractility and Ca^{2+} transient amplitude were significantly diminished in PC1 cKO cells during pacing, but they responded normally to depolarization by high K^+ when compared to cells from F/F littermates (Supplemental Figure 6J–K). Altogether, these findings suggest that shorter AP duration and alterations in SERCA activity drive perturbations in Ca^{2+} handling in PC1 cKO cardiomyocytes.

PC1 controls AP duration through its C-terminal domain

Findings reported thus far point to an unexpected role of PC1 controlling AP duration in cardiomyocytes. To begin to test for relevance to human physiology, we studied human embryonic stem cells (hESC, Supplemental Figure 7) differentiated into cardiomyocyte-like cells. Using a well-standardized protocol[19], we routinely obtain high purity populations of hESC-derived cardiomyocytes (hESC-CM), characterized by spontaneous contractions and expression of multiple cardiomyocyte markers (Figure 4A). Using these cells, we evaluated the role of PC1 in AP regulation by depleting its transcript levels using specific siRNA constructs. PC1 knockdown reduced total protein content by nearly 80% as determined by Western blot (Figure 4B). As observed in PC1 cKO adult mouse cardiomyocytes, PC1 knockdown in hESC-CM decreased AP duration measured by whole-cell current clamp (Figure 4C–G).

Our model suggests that changes in AP duration occurring in cardiomyocytes lacking PC1 drive, in part, the alterations in Ca^{2+} transient in mouse cardiomyocytes. To test that in

human cells, we performed whole-cell voltage clamp measurements on hESC-CM to determine the effect of simulated AP waveforms. We used the representative AP traces presented in Figure 4C to generate stimulus profiles to drive membrane voltage in the shape of a control or PC1-knockdown (KD) AP (applied in whole-cell voltage clamp configuration). Consistent with our hypothesis, a shorter AP (PC1-KD AP) generated a smaller Ca^{2+} transient compared to a control AP, ranging from 68–18% reduction (Figure 4H–I).

We next hypothesized that PC1 controls AP duration through its C-terminus (PC1-Ct), a region that serves as a crucial signaling effector in several cell types.[16, 20, 21] To test this, we subcloned a C-terminal fragment of PC1 under the control of the CMV promoter and packaged the construct in an adenovirus to efficiently infect hESC-CM (Figure 4J–K). PC1-Ct over-expression significantly increased AP duration in hESC-derived cardiomyocytes without affecting resting membrane potential, peak AP amplitude or maximum upstroke slope (Figure 4L–P). Altogether, these findings are consistent with a model in which PC1 regulates AP duration at the level of membrane repolarization through its C-terminus.

PC1 ablation increases outward voltage-gated K^+ currents

As cardiomyocyte repolarization depends mainly on K^+ efflux, we hypothesized that AP shortening is due to up-regulated K^+ currents. Consistent with this, using whole-cell voltage clamp we detected an increase in total outward K^+ current in PC1-deficient cardiomyocytes (Figure 5A–C). Using a tri-exponential fitting strategy to analyze K^+ current traces[22, 23] (Supplemental Figure 8), we uncovered that PC1 silencing increased I_{to}, I_{Kslow1}, I_{Kslow2} and I_{ss} in adult cardiomyocytes, without affecting their inactivation time constants (Figure 5B–C). To explore this further, we measured I_{to} directly using a voltage clamp protocol that includes a −40 mV “inactivating” prepulse, as this current is rapidly inactivated at this membrane potential.[24] Subtraction of K^+ currents without and with this “inactivating” pulse reveals I_{to} (Figure 5D). We observed increased I_{to} in PC1-deficient adult cardiomyocytes (Figure 5E). Interestingly, we did not detect differences in Ba^{2+}-sensitive I_{K1} currents between genotypes (Figure 5F–G). Together, these findings suggest that PC1 specifically affects outward voltage-gated outward Kv channels.

Next, we studied the effect of PC1 depletion on $I_{Ca,L}$ in hESC-CM. Here, consistent with our observations in PC1 cKO adult mouse cardiomyocytes, we did not observe a significant difference in steady-state activation of $I_{Ca,L}$, nor in its steady-state inactivation, in human cardiomyocytes depleted of PC1 (Supplemental Figure 9A–E). However, an increase in I_{to} was observed after PC1 ablation by siRNA (Supplemental Figure 9F). Together, this evidence suggests that PC1-deficient cardiomyocytes exhibit shorter APs. With normal LTCC, our data point to alterations in K^+ conductance, but more experiments are required as we did not measure I_{Kr}, I_{Ks} or I_{K1} in these cells.

PC1 ablation does not modify K^+ channel expression

To define mechanisms of PC1-dependent control of K^+ channel activity, we first tested for changes in channel subunit transcript abundance in freshly isolated adult cardiomyocytes harvested from F/F and PC1 cKO mice. We observed no significant differences in mRNA

levels, measured by real-time PCR, of KCND2 (Kv4.2, $I_{to,f}$), KCND3 (Kv4.3, $I_{to,f}$), KCNA4 (Kv1.4, $I_{to,s}$), KCNA5 (Kv1.5, I_{Kslow1} and I_{ss} in mice), KCNIP2 (KChIP2, regulatory β-subunit) or KCNE4 (MiRP3, regulatory β-subunit) (Supplemental Figure 10). Next, we quantified the protein abundances of Kv4.3, Kv1.4, Kv1.5, and KChIP2 in protein lysates by Western blot. Only KChIP2 showed a slight, but statistically significant, increase in protein levels in isolated adult PC1 cKO cardiomyocytes (Supplemental Figure 11). From these data, we concluded that PC1-dependent control of K^+ channel function does not occur at the level of changes in protein abundance.

PC1 inhibits Kv channels

As we did not detect meaningful differences in K^+ channel protein levels, we hypothesized that PC1 exerts its effects directly on Kv channels. To pursue this, we studied the effects of full-length PC1 (mCherry-PC1) on K^+ currents generated by heterologous Kv4.3 expression in HEK cells. Expression of Kv4.3 in HEK-293 cells resulted in transient outward K^+ currents (I_{to}) with biophysical properties similar to those observed in adult cardiomyocytes.[25] Interestingly, PC1 expression significantly decreased macroscopic Kv4.3 currents measured by whole-cell voltage clamp (Figure 6A–B), without significant effect on total Kv4.3 protein abundance (Figure 6C). In addition, we measured the effects of PC1 on Kv1.5 (I_{Kslow1}/I_{ss} in mice) and Kv2.1 (I_{Kslow2} in mice) currents in HEK cells (heterologously expressed). PC1 expression negatively regulated Kv1.5 and Kv2.1 currents without affecting total or surface levels of either channel protein (Supplemental Figure 12). These results provide evidence that PC1 acts as a negative regulator of Kv channel function, specifically Kv1.5, Kv2.1 and Kv4.3.

PC1 interacts with PC2 through a coiled-coil (CC) domain located in its C-terminal domain, serving to activate PC2 channels in lipid bilayers.[26, 27] To test whether this same region of PC1 protein participates in Kv channel inhibition, we once again employed an HEK cell system expressing a PC1 C-terminal fragment. PC1 C-terminus (PC1-Ct) expression negatively regulated Kv4.3 currents to an extent similar to that elicited by full-length PC1 (Figure 6B, D–E). Remarkably, expression of a mutant PC1-Ct lacking the CC domain (PC1-Ct ΔCC, Supplemental Figure 13) did not modify Kv4.3 currents in HEK cells, suggesting that this protein domain is required to inhibit the channel (Figure 6D–E). In addition, PC1 expression shifted the Kv4.3 steady-state inactivation curve to more negative potentials with a more pronounced slope (Supplemental Figure 14A–C), but no effects were observed when expressing its C-terminus, suggesting that PC1 effects on Kv4.3 require other domains for voltage-dependent inactivation. Surface abundance of Kv4.3, determined by a cell membrane-impermeant biotinylation assay, did not differ between PC1-Ct and PC1-Ct ΔCC, suggesting that the inhibition of Kv4.3 does not occur through altered membrane trafficking (Supplemental Figure 14).

To determine whether PC1-dependent regulation of the Kv channel takes place through direct protein-protein interaction, we first performed immunoprecipitation assays. Using a reciprocal pulldown assay, we observed that PC1 co-immunoprecipitated with Kv4.3-tGFP, and vice versa (Figure 6F) suggesting that the inhibition of Kv4.3 currents by PC1 occurs through direct protein interaction.

As noted above, PC1 interacts with PC2 through interactions between their CC domains. To gain further insight into the potential interaction between PC1 and Kv4.3, we generated an *ab initio* model of PC1-Ct (Figure 7A) using Rosetta3 software[28] and used it to model protein-protein docking against the solved structure of the cytosolic Kv4.3 N-terminal cytoplasmic domain (residues 1–143, Kv4.3 T1N helix, T1N linker and T1 domain).[29] TM score-based clustering of the *ab initio* generated models for PC1-Ct[30] led to a dominant structural ensemble, accounting for 78% of the total number of models generated (Figure 7B). The representative structural centroid of this cluster was used along the Kv4.3 N-terminal cytoplasmic domain for preliminary docking on ZDOCK[31], and the orientations of the best-scored complex were used for all-atom docking in Rosetta3. Binding energy analysis of the 100-top scoring PC1-Ct/T1 complexes (Figure 7B, Supplemental Videos 1 and 2) out of 10,000 models revealed favorable binding energy (Supplemental Table 3, Supplemental Video 3). The modeled complexes suggest that PC1-Ct potentially interacts with the cytoplasmic N-terminal domain of Kv4.3 through the nuclear localization signal (NLS), the CC region, and other unstructured regions (Figure 7C and E). The unstructured regions of PC1-Ct potentially interact through residues R4164 and R4167 with charged residues near the interdomain surface of T1 (Figure 7D–E). The NLS and the CC interact with the N-terminal helix that precedes the T1 domain (T1N helix, Figure 7C and E), a region known to be unique to Kv4 channels and important for modulation of channel currents by regulators such as KChIP.[29]

To begin to test for pathophysiological relevance in patients, we studied the impact of a *Pkd1* mutation known to cause ADPKD: exon 46: c.12682C4T, p.R4228X.[32, 33] This PC1 mutation truncates the PC1-Ct at the CC domain and abrogates interaction with PC2 in kidney epithelial cells, without affecting its localization to primary cilia.[13, 34] Using our *in silico* model of the PC1-Ct, we determined the impact of R4228X on its predicted structure and protein docking with the Kv4.3 N-terminal. Interestingly, the stop codon R4228X affected protein folding in the model (Supplemental Video 4), which potentially diminishes the amino acid residues available to stabilize the protein-protein interface, thereby reducing the docking energy with the Kv4.3 N-terminus (Supplemental Table 3).

To test this, 10,000 structures were created, and the top 100 low-energy complexes were analyzed. The average global predicted ΔΔG for PC1-Ct and Kv4.3 association was −40.2±3.5 and −30.8±2.6 R.E.U for PC1-WT and PC1-R4228X, respectively. These results suggest a reduction in interaction forces for PC1-R4228X with the Kv4.3 N-terminus. We calculated the docking energy of KChiP1 to the Kv4.3 N-terminus based on its crystal structure[29] using the same algorithm as a reference point for the interaction. Docking ΔΔG for this association was estimated to be −63.5±3.1 R.E.U, which is higher compared to PC1-Ct. Using co-immunoprecipitation, we observed that both PC1 and PC1-R4228X co-immunoprecipitated with Kv4.3-tGFP (Figure 7F) suggesting that the interaction may involve other protein regions besides the PC1-Ct.

Finally, we determined the effect of PC1 and PC1-R4228X on Kv4.3 currents, finding that only PC1 inhibited Kv4.3. The clinically relevant mutant seen in patients, PC1-R4228X, had no significant effect (Figure 7G–H), suggesting that PC1-dependent control of outward, voltage-dependent K^+ currents is perturbed in cardiomyocytes of ADPKD patients.

DISCUSSION

PC1 has been implicated in the pathogenesis of ADPKD, functioning in concert with PC2 to modulate the latter's function as a cation-permeant channel.[13] In the present study, we uncover a new role for PC1 regulating multiple members of the Kv family of voltage-gated K^+ channels. We have discovered that PC1 functions as a negative regulator of multiple channels within this family, likely due to a direct interaction between the PC1 C-terminus and Kv channel protein.

As patients with ADPKD frequently manifest cardiac pathology, we focused on the heart, identifying that PC1 ablation elicits upregulation of AP-repolarizing K^+ currents resulting in reduced AP duration and reduced SERCA activity that decrease steady-state Ca^{2+} transients. This, in turn, is manifested as impaired contractility in PC1-deficient cardiomyocytes and reduced contractile performance in PC1 cKO mice (Figure 7I). Over-expression of the PC1 C-terminus alone was sufficient to increase AP duration. Using an *ab initio* modeling strategy, we localized the potential regions of PC1-Kv4.3 channel protein-protein interaction. We observed similar effects of PC1 in hESC-CM suggesting generalizability to human physiology, although our observations are preliminary and more research is required. Finally, we determined that PC1 full length inhibits Kv4.3 channel whereas a naturally occurring human mutant ($PC1^{R4228X}$) did not. In aggregate, these findings point to an unexpected role of PC1 as a regulator of K^+ channel function and cardiomyocyte-autonomous effects of PC1 mutants in ADPKD.

Action potential repolarization in mouse and human cardiomyocytes

Our data show that PC1 ablation reduced action potential duration in both mouse adult and hESC-derived cardiomyocytes. Furthermore, PC1 ablation increased I_{to}, I_{Kslow1}, I_{Kslow2}, and I_{ss} in adult mouse cardiomyocytes, and enhanced I_{to} in human (hESC-CM) cells. We did not determine the effect of PC1 on human I_{Kr} or I_{Ks} in this study, but we hypothesize that they may be affected owing to AP duration shortening after PC1 ablation. Also, PC1 inhibited heterologously expressed human Kv4.3, Kv1.5, and Kv2.1 in HEK293 cells. Kv4.3 is expressed in both human atrial and human ventricular cardiomyocytes, whereas Kv1.5 is expressed only in human atrial cardiomyocytes.[35] Kv1.5 loss-of-function and gain-of-function have been reported in patients with atrial fibrillation.[36] As noted previously, ADPKD patients manifest elevated incidence of atrial fibrillation, which may derive either from alterations caused by renal failure or potentially via K^+ channel dysregulation within cardiomyocytes caused by dysfunctional PC1. Additional studies are required to uncover the cardiomyocyte-autonomous role(s) of PC1 mutations in the myocardial abnormalities observed in ADPKD patients.

Cardiomyocyte repolarization and function

AP duration controls the time course of $I_{Ca,L}$, SR Ca^{2+} loading and SR release, and consequently cardiomyocyte contractility.[18] We demonstrate that PC1 ablation shortens the AP in both mouse and human (hESC-CM) cardiomyocytes. Using whole-cell voltage clamp, we demonstrate that the shorter AP waveform (which mimics the AP of PC1-deficient cells) is sufficient to produce Ca^{2+} transients with decreased amplitude in both human (hESC-CM)

and mouse cardiomyocytes. In mouse cardiomyocytes, a reduction in APD_{50} caused by enhanced I_{to} will decrease LTCC mean open time, likely affecting the coupling efficiency with RyR2.[18, 37] This is supported by normal Ca^{2+} transients with square pulses at +10 mV in PC1 cKO, which suggest that the machinery for EC-coupling can be activated at normal levels with the proper time and voltage triggers. In addition, SR Ca^{2+} re-loading depends on Ca^{2+} entering via LTCC and its extrusion mainly via NCX. A reduced AP duration will limit Ca^{2+} entry and, coupled with decreased SERCA activity, will reduce SR Ca^{2+} loading in PC1 cKO cardiomyocytes, affecting Ca^{2+} homeostasis and thereby contractility.

PC1 cKO mice manifested impaired systolic and diastolic function that we find derives from APD shortening and reduced SERCA activity. It is possible that the transmural gradient of I_{to}, increasing from endocardium to epicardium and allowing for synchronization of ventricular contraction and optimization of pump function[38], could be altered by PC1 ablation.

In larger mammals such as humans, I_{to} plays a minimal role in controlling AP duration, but it is responsible for the notch in phase 1 of the AP.[39] I_{to} regulates the notch potential, allowing reactivation of $I_{Ca,L}$ at the end of phase 1 and the development of the AP plateau. At higher I_{to} currents (≈40 pA/pF for guinea pig/canine cardiomyocytes) the notch potential can depart from the activation voltage range for $I_{Ca,L}$ and suppress the AP plateau.[39]

SR Ca^{2+} release and repolarization rates have a biphasic relationship and varies significantly across species.[18] In large mammals and contrary to mouse cardiomyocytes, a physiological increase in I_{to} will increase $I_{Ca,L}$ and Ca^{2+} release.[40] Future experiments addressing the effects of PC1 on the notch potential should clarify this issue. We observed a reduction in AP duration in PC1-deficient human cardiomyocytes (hESC-CM). Our AP-clamp data suggest that shorter AP observed after PC1 silencing produces smaller Ca^{2+} transients likely resulting from reduced SR Ca^{2+} loading.[41]

PC1-dependent control of multiple Kv channels

We report that PC1 ablation up-regulates the outward K^+ currents I_{to}, I_{Kslow1}, I_{Kslow2}, and I_{ss} in adult cardiomyocytes. Consistent with these observations, PC1 is long known to govern the function of PC2, a cation channel that preferentially conducts Na^+ and K^+ relative to Ca^{2+}.[42] Further, over-expression of PC1 elicits strong inhibition of N-type Ca^{2+} channel currents and an increase of basal $GIRK_{1/2}$ K^+ currents in neurons.[43] Also, polycystins protect renal epithelial cells from mechanical stress-induced apoptosis through governance of the stretch-activated K^+-selective channel K_2P.[44]

Our model of docking between PC1-Ct and Kv4.3 points to interaction of the former with the N-terminal helix that precedes the T1 domain and the T1 domain itself (Supplemental Video 5). Importantly, this region is known to be unique to Kv4 channels and to participate in the modulation of channel currents by regulators such as KChIP.[29] Further, Kv channels harbor a conserved T1 domain that is required for tetrameric subunit formation and regulation via β-subunits which potentiate and positively regulate K^+ currents (e.g. KChIP).[45, 46] Our results suggest that PC1-Ct modulates multiple members of the Kv family,

including Kv1.5, Kv2.1 and Kv4.3 potentially through interaction with the T1 domain, possibly by disrupting the tetrameric conformation or association with KChIP.

Over-expression of full length PC1 in HEK293 cells inhibits whole-cell current carried by Kv4.3, Kv2.1, and Kv1.5 channels. Expression of the PC1 C-terminus mimicked these effects on Kv4.3. To our knowledge, we have established for the first time that PC1 is a negative regulator of voltage-gated K^+ channels of the Kv family, acting through the PC1 C-terminus.

Study limitations

As homozygous, germline silencing of *Pkd1* is embryonically lethal, we engineered cardiomyocyte-restricted knockouts. *In vitro* we used RNAi molecules specific to PC1 transcript in order to dissect its function. Evidence in ADPKD patients harboring a *Pkd1* mutation points to a relationship between PC1 protein levels and severity of disease.[12] That said, cardiac manifestations in ADPKD patients are confounded by the mutation variant, mutation severity, progressive renal failure, and ongoing left ventricular remodeling. Our findings should be interpreted with caution when extrapolating to ADPKD patients, who manifest multiple extrarenal co-morbidities, including hypertension, left ventricular hypertrophy, valvular heart disease, increased incidence of aneurysms, atrial fibrillation, and aortic dissection, among other cardiovascular manifestations.[47] ADPKD patients manifest increased incidence of cardiomyopathy.[3] LV hypertrophy and diastolic dysfunction can manifest during childhood or in young adults prior to a formal diagnosis of hypertension[5–7], and evidence suggests that LV function is impaired in ADPKD patients with normal or moderately reduced kidney function.[8] These clinical observations are consistent with the notion that cardiomyocyte-autonomous effects contribute to the cardiovascular abnormalities seen in ADPKD.

Our results demonstrate that cardiomyocyte-specific deletion of *Pkd1* impairs systolic and diastolic function in mice. However, at odds with our findings, in patients with progressive renal disease (including ADPKD) increased QT intervals and QT dispersion is associated with the reduced renal function, likely stemming from left ventricular hypertrophy.[48] As cardiomyocyte hypertrophy increases action potential duration, this could potentially explain prolonged QTs in ADPKD patients with advanced renal failure.

Our study includes data collected from mouse cardiomyocytes, cells that differ significantly from human cardiomyocytes (hESC-CM) in terms of AP duration and shape and the ion channels involved. The murine AP is shorter in duration and lacks a prominent plateau phase compared to human ventricular APs.[49] During repolarization, LTCC channels activate to maintain membrane depolarization, whereas multiple K^+ channels promote membrane repolarization. Multiple Kv channels participate in murine cardiomyocyte AP repolarization, including I_{to} ($I_{to,f}$ Kv4.3/Kv4.2, and $I_{to,s}$ Kv1.4), I_{Kslow1} (Kv1.5), I_{Kslow2} (Kv2.1), and I_{ss} (Kv1.5).[35] On the other hand, in human ventricular cardiomyocytes the Kv channels responsible for membrane repolarization are I_{to} ($I_{to,f}$ Kv4.3/Kv4.2, and $I_{to,s}$ Kv1.4), I_{Kr} (HERG, Kv11.1), I_{Ks} (KCNQ1, Kv7.1).[35] In addition, I_{KATP} is inactivated under physiological conditions, and I_{K1} participates in maintaining resting membrane potential.[35]

To address this, we studied the effects of PC1 ablation in hESC-derived cardiomyocytes, a model closer to human cardiomyocytes, but yet a cell type with immature features. For this reason, we studied cardiomyocytes after 45 days of differentiation to enhance their maturation and increase the proportion of cells with ventricular characteristics. Whereas we emphasize that similar results were observed in mouse cardiomyocytes and in hESC-derived cardiomyocytes, in terms of AP duration, additional studies are required to translate our results to ADPKD patients.

Conclusion and perspective

We have uncovered an unsuspected role of PC1 in the widespread governance of voltage-dependent K^+ channel function. As a consequence, PC1, acting as a pivotal regulator of Kv channels, participates centrally in myocyte repolarization and undoubtedly other cellular processes across numerous tissues.

Supplementary Material

Refer to Web version on PubMed Central for supplementary material.

ACKNOWLEDGMENTS

We thank Dr. José R. López (Mount Sinai Medical Center) for his insightful comments on our manuscript. Dr. Peter Harris (Division of Nephrology and Hypertension, Mayo Clinic, Rochester, Minnesota, USA) for providing the mCherry-PC1 plasmid, and Drs. Long-Sheng Song and Ang Guo (Cardiology, University of Iowa) for providing the Auto-TT analysis software.

FUNDING SOURCES

This work was supported by grants from the National Institutes of Health (HL-120732, HL-128215, HL-126012), American Heart Association (14SFRN20510023; 14SFRN20670003), Fondation Leducq (11CVD04), and Cancer Prevention and Research Institute of Texas (RP110486P3) awarded to J.A.H. FONDAP (15130011) awarded to S.L. from the Comisión Nacional de Investigación Científica y Tecnológica (CONICYT), Santiago, Chile. This research was partially supported by the super-computing infrastructure of the National Laboratory for High Performance Computing NLHPC (ECM-02), and by NVIDIA Corporation through the donation of the Titan X and XP GPUs used in this work (C.A.R.S.). F.A. was supported by a Postdoctoral Fellowship (16POST30680016) and S.Y.K. by a Predoctoral Fellowship (16PRE29660003) from the American Heart Association (AHA). G.G.S. was supported by grants from the AHA and the Theodore and Beulah Beasley Foundation (18POST34060230). K.M.F. and D.T. were supported by Postdoctoral Fellowships (F32HL136151 and F32HL142244, respectively) from the National Heart, Lung, and Blood Institute of the National Institutes of Health.

REFERENCES

1. Bergmann C, Guay-Woodford LM, Harris PC, Horie S, Peters DJM and Torres VE. Polycystic kidney disease. Nat Rev Dis Primers. 2018;4:50. [PubMed: 30523303]
2. Torres VE, Harris PC and Pirson Y. Autosomal dominant polycystic kidney disease. Lancet. 2007;369:1287–1301. [PubMed: 17434405]
3. Chebib FT, Hogan MC, El-Zoghby ZM, Irazabal MV, Senum SR, Heyer CM, Madsen CD, Cornec-Le Gall E, Behfar A, Harris PC and Torres VE. Autosomal Dominant Polycystic Kidney Patients May Be Predisposed to Various Cardiomyopathies. Kidney Int Rep. 2017;2:913–923. [PubMed: 29270497]
4. Schrier RW, Abebe KZ, Perrone RD, Torres VE, Braun WE, Steinman TI, Winklhofer FT, Brosnahan G, Czarnecki PG, Hogan MC, Miskulin DC, Rahbari-Oskoui FF, Grantham JJ, Harris PC, Flessner MF, Bae KT, Moore CG, Chapman AB and Investigators H-PT. Blood pressure in early autosomal dominant polycystic kidney disease. N Engl J Med. 2014;371:2255–2266. [PubMed: 25399733]

5. Cadnapaphornchai MA, McFann K, Strain JD, Masoumi A and Schrier RW. Increased left ventricular mass in children with autosomal dominant polycystic kidney disease and borderline hypertension. Kidney Int. 2008;74:1192–1196. [PubMed: 18716604]
6. Oflaz H, Alisir S, Buyukaydin B, Kocaman O, Turgut F, Namli S, Pamukcu B, Oncul A and Ecder T. Biventricular diastolic dysfunction in patients with autosomal-dominant polycystic kidney disease. Kidney Int. 2005;68:2244–2249. [PubMed: 16221225]
7. Zeier M, Geberth S, Schmidt KG, Mandelbaum A and Ritz E. Elevated blood pressure profile and left ventricular mass in children and young adults with autosomal dominant polycystic kidney disease. J Am Soc Nephrol. 1993;3:1451–1457. [PubMed: 8490116]
8. Spinelli L, Pisani A, Giugliano G, Trimarco B, Riccio E, Visciano B, Remuzzi G, Ruggenenti P and Group AL-CS. Left ventricular dysfunction in ADPKD and effects of octreotide-LAR: A cross-sectional and longitudinal substudy of the ALADIN trial. Int J Cardiol. 2019;275:145–151. [PubMed: 30509370]
9. Criollo A, Altamirano F, Pedrozo Z, Schiattarella GG, Li DL, Rivera-Mejias P, Sotomayor-Flores C, Parra V, Villalobos E, Battiprolu PK, Jiang N, May HI, Morselli E, Somlo S, de Smedt H, Gillette TG, Lavandero S and Hill JA. Polycystin-2-dependent control of cardiomyocyte autophagy. J Mol Cell Cardiol. 2018;118:110–121. [PubMed: 29518398]
10. Anyatonwu GI, Estrada M, Tian X, Somlo S and Ehrlich BE. Regulation of ryanodine receptor-dependent calcium signaling by polycystin-2. Proc Natl Acad Sci U S A. 2007;104:6454–6459. [PubMed: 17404231]
11. Paavola J, Schliffke S, Rossetti S, Kuo IY, Yuan S, Sun Z, Harris PC, Torres VE and Ehrlich BE. Polycystin-2 mutations lead to impaired calcium cycling in the heart and predispose to dilated cardiomyopathy. J Mol Cell Cardiol. 2013;58:199–208. [PubMed: 23376035]
12. Ong AC and Harris PC. A polycystin-centric view of cyst formation and disease: the polycystins revisited. Kidney Int. 2015;88:699–710. [PubMed: 26200945]
13. Hanaoka K, Qian F, Boletta A, Bhunia AK, Piontek K, Tsiokas L, Sukhatme VP, Guggino WB and Germino GG. Co-assembly of polycystin-1 and −2 produces unique cation-permeable currents. Nature. 2000;408:990–994. [PubMed: 11140688]
14. Delling M, Indzhykulian AA, Liu X, Li Y, Xie T, Corey DP and Clapham DE. Primary cilia are not calcium-responsive mechanosensors. Nature. 2016;531:656–660. [PubMed: 27007841]
15. Padovano V, Podrini C, Boletta A and Caplan MJ. Metabolism and mitochondria in polycystic kidney disease research and therapy. Nat Rev Nephrol. 2018;14:678–687. [PubMed: 30120380]
16. Pedrozo Z, Criollo A, Battiprolu PK, Morales CR, Contreras-Ferrat A, Fernandez C, Jiang N, Luo X, Caplan MJ, Somlo S, Rothermel BA, Gillette TG, Lavandero S and Hill JA. Polycystin-1 is a cardiomyocyte mechanosensor that governs L-type Ca2+ channel protein stability. Circulation. 2015;131:2131–2142. [PubMed: 25888683]
17. Guo A and Song LS. AutoTT: automated detection and analysis of T-tubule architecture in cardiomyocytes. Biophys J. 2014;106:2729–2736. [PubMed: 24940790]
18. Sah R, Ramirez RJ, Oudit GY, Gidrewicz D, Trivieri MG, Zobel C and Backx PH. Regulation of cardiac excitation-contraction coupling by action potential repolarization: role of the transient outward potassium current (I(to)). J Physiol. 2003;546:5–18. [PubMed: 12509475]
19. Burridge PW, Matsa E, Shukla P, Lin ZC, Churko JM, Ebert AD, Lan F, Diecke S, Huber B, Mordwinkin NM, Plews JR, Abilez OJ, Cui B, Gold JD and Wu JC. Chemically defined generation of human cardiomyocytes. Nat Methods. 2014;11:855–860. [PubMed: 24930130]
20. Chauvet V, Tian X, Husson H, Grimm DH, Wang T, Hiesberger T, Igarashi P, Bennett AM, Ibraghimov-Beskrovnaya O, Somlo S and Caplan MJ. Mechanical stimuli induce cleavage and nuclear translocation of the polycystin-1 C terminus. J Clin Invest. 2004;114:1433–1443. [PubMed: 15545994]
21. Lal M, Song X, Pluznick JL, Di Giovanni V, Merrick DM, Rosenblum ND, Chauvet V, Gottardi CJ, Pei Y and Caplan MJ. Polycystin-1 C-terminal tail associates with beta-catenin and inhibits canonical Wnt signaling. Hum Mol Genet. 2008;17:3105–3117. [PubMed: 18632682]
22. Liu J, Kim KH, London B, Morales MJ and Backx PH. Dissection of the voltage-activated potassium outward currents in adult mouse ventricular myocytes: I(to,f), I(to,s), I(K,slow1), I(K,slow2), and I(ss). Basic Res Cardiol. 2011;106:189–204. [PubMed: 21253754]

23. Wang Y, Cheng J, Chen G, Rob F, Naseem RH, Nguyen L, Johnstone JL and Hill JA. Remodeling of outward K+ currents in pressure-overload heart failure. J Cardiovasc Electrophysiol. 2007;18:869–875. [PubMed: 17537202]
24. Brouillette J, Clark RB, Giles WR and Fiset C. Functional properties of K+ currents in adult mouse ventricular myocytes. J Physiol. 2004;559:777–798. [PubMed: 15272047]
25. Faivre JF, Calmels TP, Rouanet S, Javre JL, Cheval B and Bril A. Characterisation of Kv4.3 in HEK293 cells: comparison with the rat ventricular transient outward potassium current. Cardiovasc Res. 1999;41:188–199. [PubMed: 10325966]
26. Casuscelli J, Schmidt S, DeGray B, Petri ET, Celic A, Folta-Stogniew E, Ehrlich BE and Boggon TJ. Analysis of the cytoplasmic interaction between polycystin-1 and polycystin-2. Am J Physiol Renal Physiol. 2009;297:F1310–F1315. [PubMed: 19726544]
27. Xu GM, Gonzalez-Perrett S, Essafi M, Timpanaro GA, Montalbetti N, Arnaout MA and Cantiello HF. Polycystin-1 activates and stabilizes the polycystin-2 channel. J Biol Chem. 2003;278:1457–1462. [PubMed: 12407099]
28. Bender BJ, Cisneros A 3rd, Duran AM, Finn JA, Fu D, Lokits AD, Mueller BK, Sangha AK, Sauer MF, Sevy AM, Sliwoski G, Sheehan JH, DiMaio F, Meiler J and Moretti R. Protocols for Molecular Modeling with Rosetta3 and RosettaScripts. Biochemistry. 2016;55:4748–4763. [PubMed: 27490953]
29. Pioletti M, Findeisen F, Hura GL and Minor DL Jr. Three-dimensional structure of the KChIP1-Kv4.3 T1 complex reveals a cross-shaped octamer. Nat Struct Mol Biol. 2006;13:987–995. [PubMed: 17057713]
30. Hung LH and Samudrala R. fast_protein_cluster: parallel and optimized clustering of large-scale protein modeling data. Bioinformatics. 2014;30:1774–1776. [PubMed: 24532722]
31. Pierce BG, Wiehe K, Hwang H, Kim BH, Vreven T and Weng Z. ZDOCK server: interactive docking prediction of protein-protein complexes and symmetric multimers. Bioinformatics. 2014;30:1771–1773. [PubMed: 24532726]
32. Paul BM, Consugar MB, Ryan Lee M, Sundsbak JL, Heyer CM, Rossetti S, Kubly VJ, Hopp K, Torres VE, Coto E, Clementi M, Bogdanova N, de Almeida E, Bichet DG and Harris PC. Evidence of a third ADPKD locus is not supported by re-analysis of designated PKD3 families. Kidney Int. 2014;85:383–392. [PubMed: 23760289]
33. Turco AE, Clementi M, Rossetti S, Tenconi R and Pignatti PF. An Italian family with autosomal dominant polycystic kidney disease unlinked to either the PKD1 or PKD2 gene. Am J Kidney Dis. 1996;28:759–761. [PubMed: 9158217]
34. Cai Y, Fedeles SV, Dong K, Anyatonwu G, Onoe T, Mitobe M, Gao JD, Okuhara D, Tian X, Gallagher AR, Tang Z, Xie X, Lalioti MD, Lee AH, Ehrlich BE and Somlo S. Altered trafficking and stability of polycystins underlie polycystic kidney disease. J Clin Invest. 2014;124:5129–5144. [PubMed: 25365220]
35. Huang CL. Murine electrophysiological models of cardiac arrhythmogenesis. Physiol Rev. 2017;97:283–409. [PubMed: 27974512]
36. Schmitt N, Grunnet M and Olesen SP. Cardiac potassium channel subtypes: new roles in repolarization and arrhythmia. Physiol Rev. 2014;94:609–653. [PubMed: 24692356]
37. Kaprielian R, Sah R, Nguyen T, Wickenden AD and Backx PH. Myocardial infarction in rat eliminates regional heterogeneity of AP profiles, I(to) K(+) currents, and [Ca(2+)](i) transients. Am J Physiol Heart Circ Physiol. 2002;283:H1157–H1168. [PubMed: 12181147]
38. Zicha S, Xiao L, Stafford S, Cha TJ, Han W, Varro A and Nattel S. Transmural expression of transient outward potassium current subunits in normal and failing canine and human hearts. J Physiol. 2004;561:735–748. [PubMed: 15498806]
39. Dong M, Sun X, Prinz AA and Wang HS. Effect of simulated I(to) on guinea pig and canine ventricular action potential morphology. Am J Physiol Heart Circ Physiol. 2006;291:H631–H637. [PubMed: 16565319]
40. Sah R, Ramirez RJ and Backx PH. Modulation of Ca(2+) release in cardiac myocytes by changes in repolarization rate: role of phase-1 action potential repolarization in excitation-contraction coupling. Circ Res. 2002;90:165–173. [PubMed: 11834709]

41. Bassani RA, Altamirano J, Puglisi JL and Bers DM. Action potential duration determines sarcoplasmic reticulum Ca2+ reloading in mammalian ventricular myocytes. J Physiol. 2004;559:593–609. [PubMed: 15243136]

42. Shen PS, Yang X, DeCaen PG, Liu X, Bulkley D, Clapham DE and Cao E. The structure of the polycystic kidney disease channel PKD2 in lipid nanodiscs. Cell. 2016;167:763–773 e11. [PubMed: 27768895]

43. Delmas P, Nomura H, Li X, Lakkis M, Luo Y, Segal Y, Fernandez-Fernandez JM, Harris P, Frischauf AM, Brown DA and Zhou J. Constitutive activation of G-proteins by polycystin-1 is antagonized by polycystin-2. J Biol Chem. 2002;277:11276–11283. [PubMed: 11786542]

44. Peyronnet R, Sharif-Naeini R, Folgering JH, Arhatte M, Jodar M, El Boustany C, Gallian C, Tauc M, Duranton C, Rubera I, Lesage F, Pei Y, Peters DJ, Somlo S, Sachs F, Patel A, Honore E and Duprat F. Mechanoprotection by polycystins against apoptosis is mediated through the opening of stretch-activated K(2P) channels. Cell Rep. 2012;1:241–250. [PubMed: 22832196]

45. Long SB, Campbell EB and Mackinnon R. Crystal structure of a mammalian voltage-dependent Shaker family K+ channel. Science. 2005;309:897–903. [PubMed: 16002581]

46. Miller C An overview of the potassium channel family. Genome Biol. 2000;1:REVIEWS0004. [PubMed: 11178226]

47. Krishnappa V, Vinod P, Deverakonda D and Raina R. Autosomal dominant polycystic kidney disease and the heart and brain. Cleve Clin J Med. 2017;84:471–481. [PubMed: 28628430]

48. Stewart GA, Gansevoort RT, Mark PB, Rooney E, McDonagh TA, Dargie HJ, Stuart R, Rodger C and Jardine AG. Electrocardiographic abnormalities and uremic cardiomyopathy. Kidney Int. 2005;67:217–226. [PubMed: 15610245]

49. Boukens BJ, Rivaud MR, Rentschler S and Coronel R. Misinterpretation of the mouse ECG: ‘musing the waves of Mus musculus’. J Physiol. 2014;592:4613–4626. [PubMed: 25260630]

Clinical Perspective

What is new?

- PC1 regulates basal cardiac function, and its loss-of-function elicits both systolic and diastolic dysfunction.
- PC1 ablation reduces cardiomyocyte action potential duration, whereas PC1 C-terminus over-expression has the opposite effect.
- PC1 regulates multiple potassium channels involved in cardiomyocyte repolarization in a manner that may involve direct protein-protein interactions.
- PC1-deficient cardiomyocytes exhibit reduced sarcoplasmic reticulum Ca^{2+} stores and decreased SERCA activity.

What are the clinical implications?

- Loss-of-function mutations in the *Pkd1* gene, as occurs in ADPKD patients, directly impairs cardiomyocyte electrical activity, Ca^{2+}-handling and contractile function, independent of the associated co-morbidities seen in these patients.

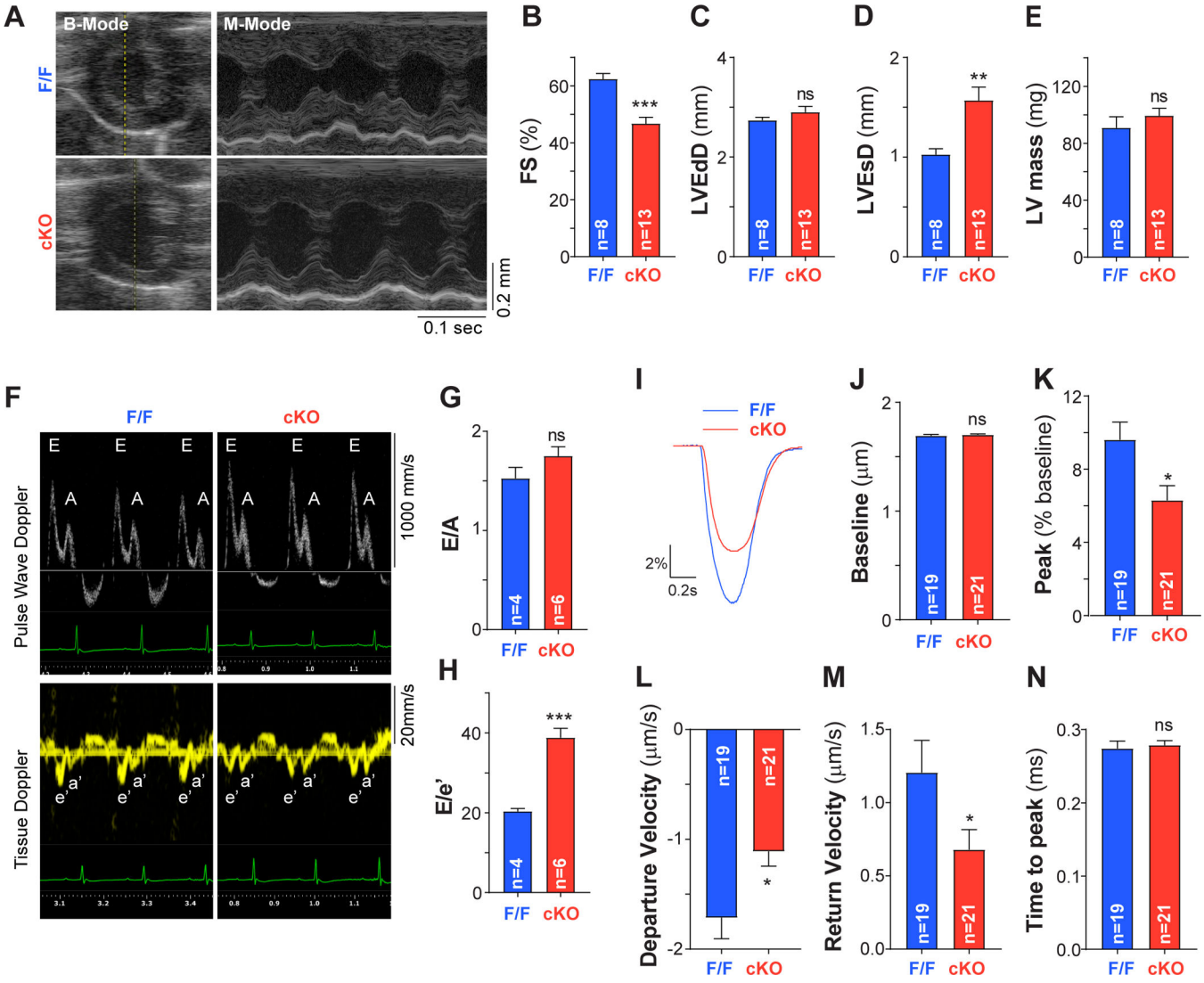

Figure 1: Systolic and diastolic contractile function are reduced upon cardiomyocyte-specific PC1 ablation.

A. Representative B- and M-mode echocardiograms in a conscious mouse (8–16-week-old). **B.** Contractile performance quantified as percentage fractional shortening [FS (%)] revealed reduced systolic function in PC1 cKO (cKO) compared to control mice (F/F). **C.** LVEdD, left ventricular end-diastolic diameter. **D.** LVESD, left ventricular end-systolic diameter. **E.** left ventricular (LV) mass. **F.** Representative pulse wave and tissue doppler recordings in anesthetized mice to measure diastolic function as E/A and E/e' ratios (**G-H**). Impaired diastolic function was observed in PC1 cKO mice. Data were obtained from "n" different mice, indicated at the bottom of each bar. $^{**}P<0.01$;$^{***}P<0.001$; ns: non-significant differences; compared to F/F. Unpaired *t* test. **I.** Representative contractility traces obtained using an IonOptix imaging system during pacing at 0.5 Hz in adult cardiomyocytes isolated from F/F and PC1 cKO (cKO) mice. **J-N.** Quantification of baseline sarcomere length, peak of contraction, maximum velocities and time to peak from the contractility traces. Reduced contractility with slower kinetics of both contraction and relaxation were observed in adult

PC1 cKO cardiomyocytes. *P<0.05; ns: non-significant differences; compared to F/F. Unpaired t test.

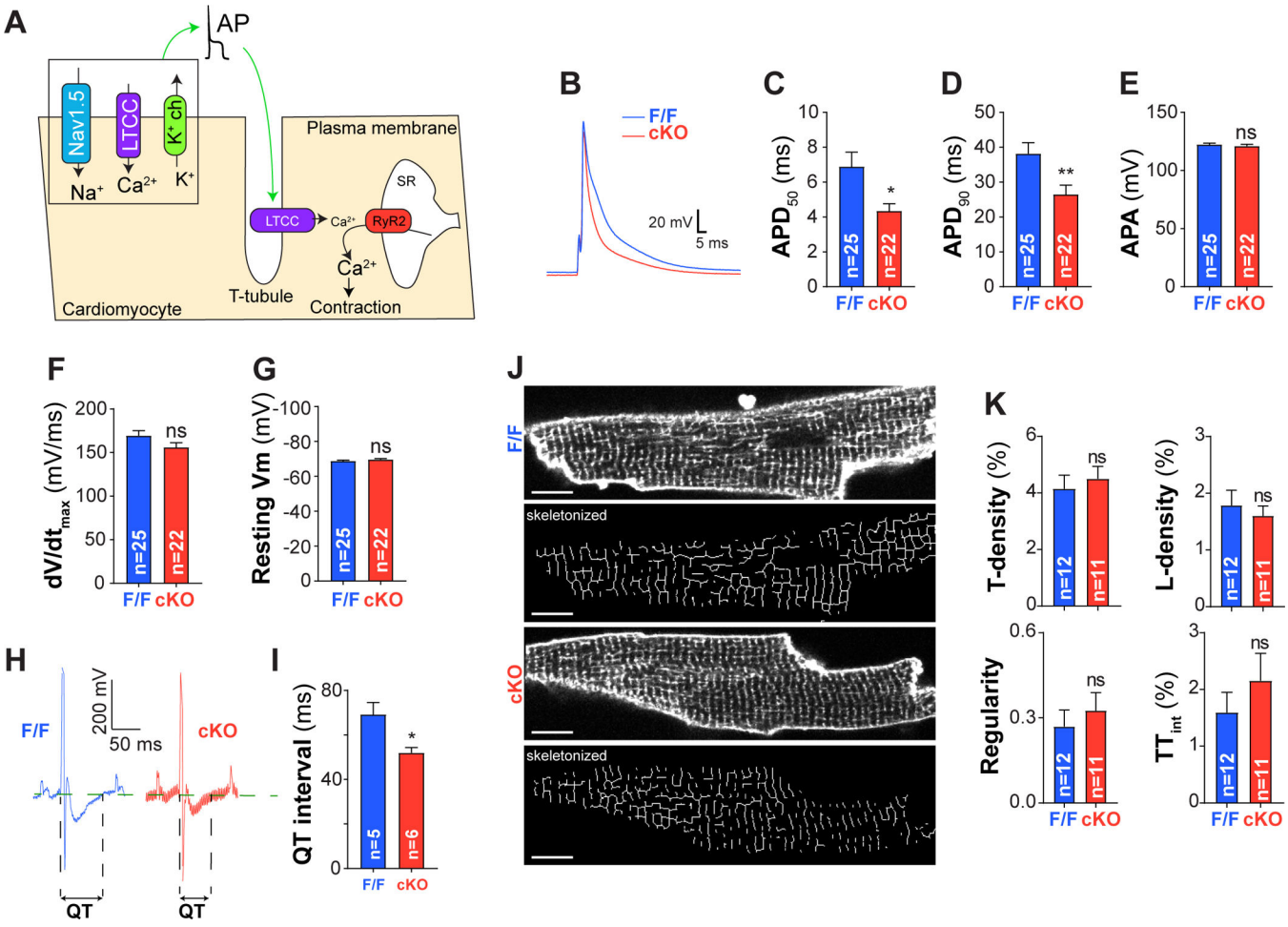

Figure 2: Cardiomyocyte action potential is impaired in adult PC1 cKO cardiomyocytes.

A. Schematic illustrating the ECC process. An action potential (AP) propagates into the cardiomyocyte T-tubule network promoting LTCC-dependent Ca^{2+} entry. This influx in Ca^{2+} triggers RyR2 activation (located at the sarcoplasmic reticulum SR) and a subsequent massive Ca^{2+} release occurs to elicit contraction. **B.** Representative AP traces obtained by whole-cell current clamp (intracellular solution contained 5 mM EGTA).**C-D.** AP duration at 50 and 90% repolarization (APD_{50} and APD_{90}), revealing reduced AP duration upon PC1 ablation. **E.** AP amplitude (APA, absolute values), **F.** Maximum upstroke slope (dV/dt_{max}) and (**G**) resting membrane potential (Vm) for both adult F/F and PC1 cKO cardiomyocytes **H.** Representative electrocardiogram demonstrating reduced QT interval (**I**) in cKO mice. **J.** T-tubule network assessed by FluoVolt and confocal microscopy. Scale bar = 10 μm. **K.** T- and L-tubule density (T- and L-density), global T-tubule regularity and T-tubule integrity (TT_{int}) were measured with AutoTT software and expressed as described.[17] No differences in T-tubule network were observed in PC1-deficient cardiomyocytes (PC1 cKO). Data were obtained from at least three different cultures for each genotype, and "n=cells" are indicated at the bottom of each bar. *P<0.05; **P<0.01; ns: non-significant differences; compared to F/F. Unpaired t test.

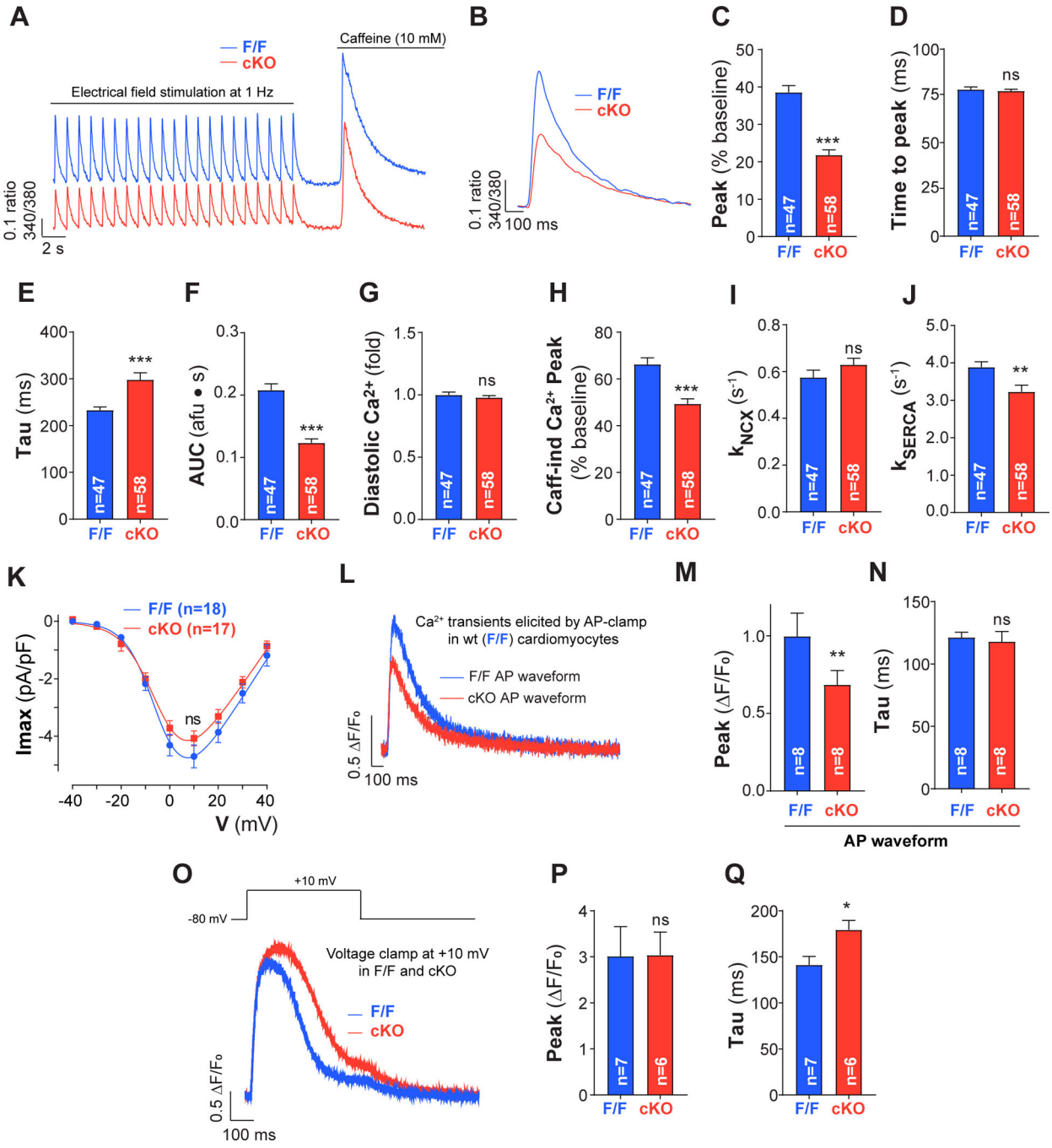

Figure 3: Ca^{2+} cycling is reduced in PC1-deficient adult cardiomyocytes.

A. Cardiomyocytes were electrically stimulated at 1 Hz until reaching steady state (25–30 times) and then caffeine 10 mM was quickly perfused to assess SR Ca^{2+} stores in adult cardiomyocytes isolated from F/F and PC1 cKO mice. Ca^{2+} transients were measured using Fura-2AM and IonOptix. **B.** Representative Fura-2AM fluorescence (ratio excitation 340/380nm) for pacing at 1 Hz (average of the 10 last transients before caffeine). **C-G.** Fura-2 fluorescence transient peak amplitude, time to peak, time constant of decay (tau), area under the curve (AUC) and diastolic Ca^{2+} levels. A reduced Ca^{2+} amplitude was

observed in PC1 cKO cardiomyocytes. **H.** Caffeine-induced (Caff-ind) Ca^{2+} transient peak amplitude after pacing. Data suggest that SR Ca^{2+} stores are reduced in PC1 cKO after pacing. **I-J.** NCX and SERCA activities (kNCX and kSERCA) calculated using the decay rates for transients elicited at 1 Hz and caffeine. **K.** LTCC steady-state activation measured by whole-cell voltage clamp (Imax, maximum current; V, voltage). **L.** Representative data from Figure 2B were used to generate voltage stimulus profiles for whole-cell voltage clamp mimicking a F/F and PC1 cKO AP waveform. AP-clamp was performed in WT cardiomyocytes using the different waveforms in the same cell and Ca^{2+} measured with Fluo-4 loaded from the patch pipette. AP-clamp stimulation was at 1 Hz and 20 consecutive responses of Ca^{2+} transients were recorded; last 5 transients were averaged and analyzed. **M-N.** PC1 cKO AP waveforms produced smaller Ca^{2+} transients compared to F/F AP waveforms in control cardiomyocytes. **O-Q.** Ca^{2+} transients (Fluo-4) elicited by square pulses (20 pulses at +10 mV for 500ms at 1 Hz) under whole-cell voltage clamp and their quantification (beats 15–20) in both F/F and PC1 cKO cardiomyocytes. Data were obtained from at least three different cultures for each genotype, and “n=cells” are indicated at the bottom of each bar. *P<0.05; **P<0.01; ***P<0.001 ns: non-significant differences; compared to F/F. Unpaired t-test (except for M-N, paired t-test).

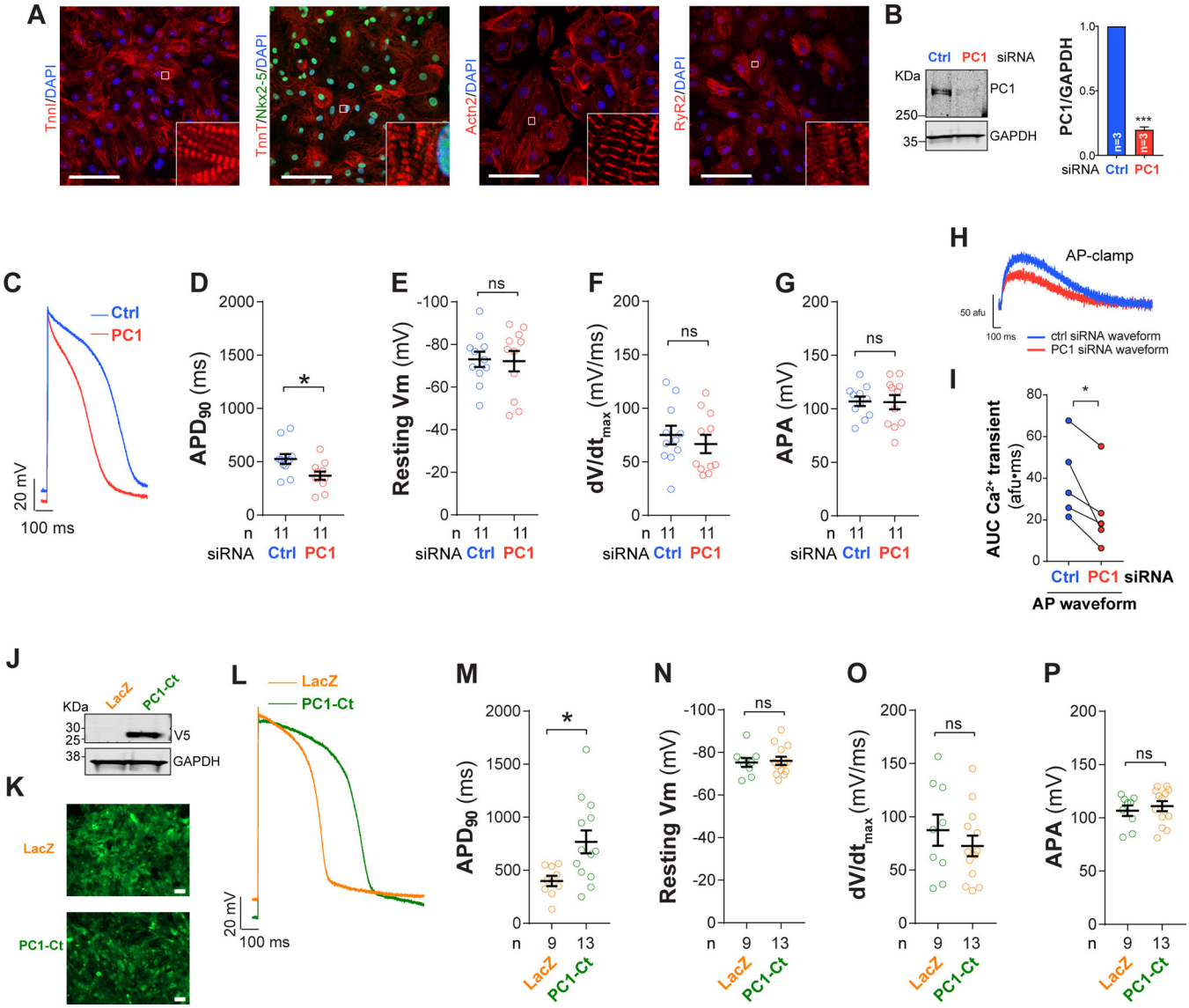

Figure 4: PC1 controls AP duration in human embryonic stem cell derived cardiomyocytes (hESC-CM).

A. Representative immunostainings for TnnI, Actn2, TnT, Nkx2–5, and RyR2 in hESC-CM (Bar = 100 μm). **B.** Knockdown using siRNA reduces PC1 protein by 80%. Using whole-cell current clamp, we observed a reduction in AP duration (APD_{90}) in PC1-deficient cardiomyocytes (**C-D**) (intracellular solution contained 100 nM Ca^{2+}). **E.** Resting membrane potential (Vm). **F.** Maximum upstroke slope (dV/dt_{max}). **G.** AP amplitude (APA, absolute values). For whole-cell current clamp, current injection was delivered at 0.5Hz frequency to generate an AP. **H-I.** Representative data from **C** were used to generate voltage stimulus profiles for whole-cell voltage clamp mimicking a control and PC1-knockdown (KD) AP from a holding potential of −80 mV. AP stimulation was at 0.5 Hz and 5 consecutive responses of Ca^{2+} transients were averaged. PC1-KD AP waveforms produced smaller Ca^{2+} transients compared to Ctrl AP (**I**, AUC, area under the curve). **J.** Adenovirus-mediated over-expression of LacZ or PC1-Ct in hESC-CM (co-expressing Zsgreen1). Representative

Western blot for the V5-tag contained in PC1-Ct and GAPDH as loading control. **K.** Zsgreen1 fluorescence images demonstrate high transduction efficiency in hESC-CM after adenoviral infection. **L.** APs measured using whole-cell current clamp in hESC-CM. An increase in AP duration (APD_{90}) was observed upon PC1-Ct over-expression (**M**), without alterations in resting membrane potential (Vm), maximum upstroke slope (dV/dt_{max}) or AP amplitude (APA, absolute values) (**N-P**). Data were obtained from at least three different cultures for each condition, and "n=cells" are indicated at the bottom of each bar. *P<0.05; ***P<0.001; ns: non-significant differences; compared to Ctrl siRNA or LacZ. Unpaired t-test (except for **H-I**, paired t-test, experiments in the same cell).

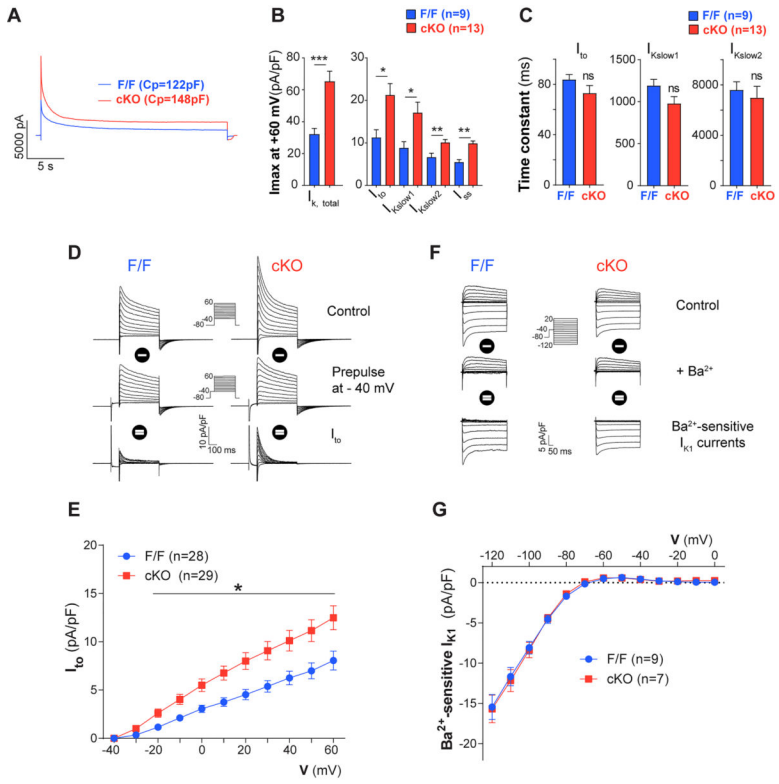

Figure 5: Increased outward K^+ currents in PC1 cKO cardiomyocytes.

Total maximum K^+ current elicited at +60 mV for 25 s measured by whole-cell voltage clamp in adult cardiomyocytes obtained from F/F and cKO mice. Tri-exponential fitting from K^+ current revealed increased I_{to}, I_{Kslow1}, I_{Kslow2}, and I_{ss} maximum currents in PC1-deficient cardiomyocytes (**A-B**) with no difference in exponential decay time constants (**C**). **D-E**. I_{to} recordings in adult cardiomyocytes. Recordings were obtained using a pre-step at −40 mV for 500 ms to inactivate I_{to}. **D.** Representative traces and I_{to} measurements in F/F and cKO adult cardiomyocytes. **E.** Quantification of I_{to} maximum currents. **F-G.** Ba^{2+}-sensitive I_{K1} currents revealed after the addition of 100 μM Ba^{2+} in both F/F and PC1 cKO cardiomyocytes. **G.** Quantification of I_{k1} current. Data were obtained from at least three different cultures for each genotype, and "n=cells" are indicated at the bottom of each bar. * P<0.05; ** P<0.01, *** P<0.001; ns: non-significant differences; compared to F/F. Unpaired t-test.

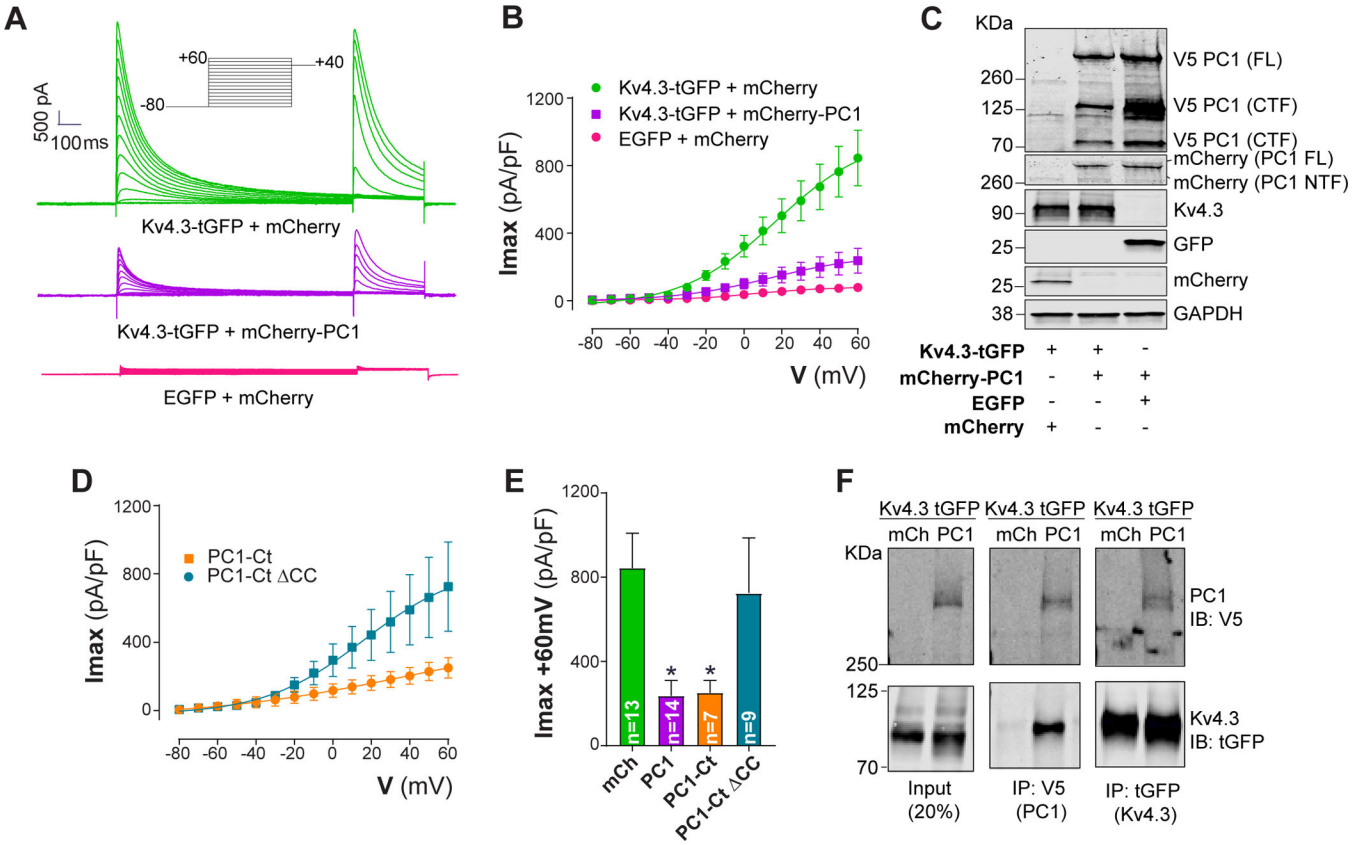

Figure 6: PC1 inhibits Kv4.3 through its C-terminal coiled-coil (CC) domain.

HEK-293T cells were transiently transfected with plasmids encoding Kv4.3-tGFP, mCherry-PC1-V5 (full length PC1; V5 tag), mCherry and EGFP. **A.** Representative traces of Kv4.3 currents measured with whole-cell voltage clamp. **B.** I-V curves for Kv4.3 demonstrating the inhibitory effect of PC1 (Imax, maximum current; V, voltage). **C.** Western blot analysis revealed no differences in Kv4.3 elicited by PC1 co-expression. PC1 protein undergo cleavage at multiple sites. PC1 full-length (FL), C-terminal fragments (CTF), N-terminal fragments (NTF). **D.** We evaluated the effect of PC1-Ct and its CC domain on Kv4.3 currents. IV curves illustrate the inhibitory effect of PC1-Ct (similar to full length PC1), whereas PC1-Ct lacking the CC domain (PC1-Ct ΔCC) had no effect. **E.** Quantification of Kv4.3 maximum currents (I_{max}) at +60 mV (from panels **B** and **D**). **F.** The co-immunoprecipitation analysis demonstrated a potential interaction between Kv4.3 and PC1. HEK cells were transfected with Kv4.3-tGFP and either mCherry or mCherry-PC1-V5. IP, immunoprecipitation, IB; immunoblot. Data were obtained from at least three different cultures for each condition, and "n=cells" are indicated in each graph. **P*<0.05; compared to mCh. ANOVA with Dunnett post hoc test.

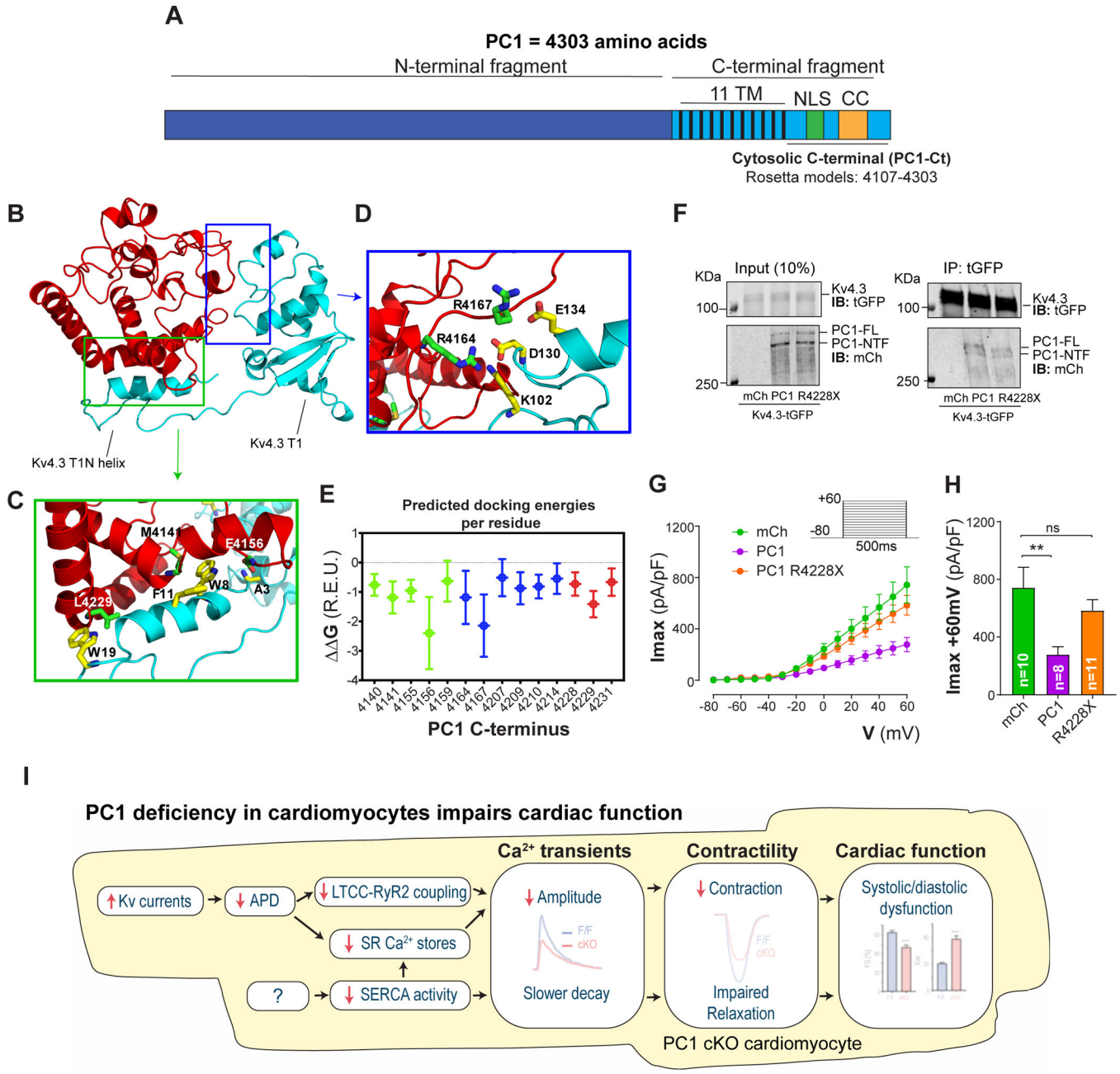

Figure 7: PC1 C-terminus modelling and docking with Kv4.3 N-terminal domain.

A. PC1 protein showing both the N- and C-terminal fragments. PC1 cytosolic C-terminus (amino acids 4107–4303) was used for *ab initio* modeling. TM: transmembrane domain, NLS: nuclear localization signal, CC: Coiled-coil domain, R4228X: PC1 mutation localized within the CC. **B.** Modeled complex between PC1-Ct and Kv4.3 N-terminal cytoplasmic domain (Kv4.3 T1N helix, T1N linker and T1 domain). Representative structure of the lowest-energy complex for PC1-Ct (red) bound to Kv4.3 N-terminus (residues 1–143, Protein Data Bank (PDB) ID: 2I2R, chain L, cyan). Two sites of interaction were identified, one with the T1N helix (**C**, site 1, green box) and another with the T1 domain itself (**D**, site 2, blue box). Interactions between residues from PC1-Ct (green sticks) and Kv4.3 (yellow

sticks) are shown for both site 1 (**C**) and site 2 (**D**). Only residues with an energy contribution < -1 Rosetta energy units (R.E.U) are shown. **E**. Estimated per residue energetic contributions for 100 lowest-energy structures modeled using Rosetta. NLS residues are shown in green, CC residues in red and other regions in blue. Error bars correspond to the standard deviation among all 100 predicted structures. **F.** Co-immunoprecipitation between Kv4.3 and mCh, PC1 and PC1 R4228X. Kv4.3 was able to pull down both PC1 (full length) and PC1 R4228X. **G-H.** Representative traces and quantification of Kv4.3 currents measured with whole-cell voltage clamp, showing the inhibitory effect of PC1, whereas PC1 R4228X had no effect. Data were obtained from at least three different cultures for each condition, and "n=cells" are indicated in each graph. ** P<0.01ns: non-significant differences. ANOVA with Dunnett post hoc test. **I.** Based on our experimental data, we propose a model in which PC1 controls cardiac repolarization and action potential duration through modulation of Kv channels. Shorter AP duration (APD) impairs LTCC-RyR2 coupling (affecting $I_{Ca,L}$ mean open time)[18] and reduces SR Ca^{2+} loading, which is further aggravated by reduced SERCA activity. Altogether, these results reveal that PC1 regulates Ca^{2+} cycling and contractility in adult cardiomyocytes.